ACS Catalysis

Research Article

pubs.acs.org/acscatalysis

Development of the CON-type Aluminosilicate Zeolite and Its Catalytic Application for the MTO Reaction

Masato Yoshioka, Toshiyuki Yokoi,* and Takashi Tatsumi

Chemical Resources Laboratory, Tokyo Institute of Technology, 4259 Nagatsuta, Midori-ku, Yokohama 226-8503, Japan

Supporting Information

ABSTRACT: The **CON**-type aluminosilicate zeolites, which consist of a three-dimensional pore system with 12-, 12-, and 10-membered ring pores have been prepared by postsynthesis and the newly developed direct-synthesis methods. We first found that the **CON**-type aluminosilicate zeolites exhibited a higher catalytic performance in the methanol to olefins (MTO) reaction in terms of duration and propene selectivity than the **MFI** and ***BEA**-type aluminosilicate zeolites. They exhibited high propene selectivity, low ethene selectivity, and a very long catalytic life compared to Beta and ZSM-5; the selectivity for C3−C4 olefins reached 80%. Interestingly, the **CON**-type aluminosilicate zeolite synthesized by the direct-synthesis method showed a much longer catalytic lifetime than the one obtained by the postsynthesis method. The ^{27}Al MAS and ^{27}Al MQMAS NMR spectra suggest that there is a significant difference in the state of tetrahedrally coordinated Al species between the directly and postsynthesized zeolites, leading to the marked difference in the catalytic performance.

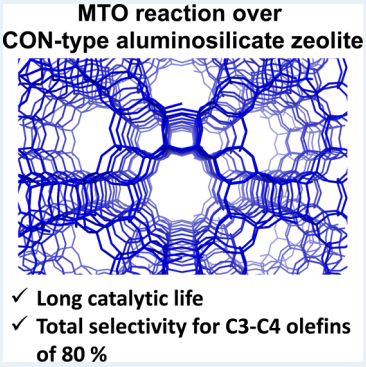

KEYWORDS: *CON-type zeolite, aluminosilicate, direct synthesis, postsynthesis, MTO reaction, Al distribution in the framework*

1. INTRODUCTION

The Methanol To Olefins (MTO) reaction becomes highly important for producing lower olefins as important basic chemicals for the polymer industry instead of steam cracking of naphtha.[1−3] Various zeolites have been examined for the MTO reaction; there are numerous reports on the modifications of catalysts to promote the transformation of methanol to olefins and to control the selectivity to the desired products.[4−14] To date, ZSM-5, SAPO-34, and SSZ-13 have been well-known as excellent catalysts for the MTO reaction.[4,5]

Nowadays, due to the augmentation of production of ethene from ethane in the Middle East, fundamental chemical feedstock required by the chemical industry is shifting from C2−C3 to C3−C4 olefins. The development of the zeolite catalysts that can selectively produce C3−C4 olefins by the conversion of methanol has been strongly desired. Since zeolites having small pores do not meet this demand, we have adopted aluminosilicate zeolite having 12MR channels as catalysts for the MTO reaction to achieve a high selectivity to C3−C4 olefins and a long catalytic life. Actually, faujasite (**FAU**), beta (***BEA**), and MCM-68 (**MSE**) zeolites were examined in the catalytic activity in the MTO reaction.[15] However, the **CON**-type zeolite, which consists of a three-dimensional channel system with 12-, 12-, and 10-MR pores, as a catalyst for the MTO reaction has attracted little attention to date. We have discovered a unique catalytic performance of the **CON**-type zeolites in the MTO reaction.

In 1993, SSZ-26 and SSZ-33, which are high-silica molecular sieves containing a three-dimensional pore system comprised of intersecting 10- and 12-ring pores, were developed.[16] They are a family of the **CON**-type zeolite, but their structures consist of the stacking of polymorphs A and B.[17] The first report on the synthesis of the zeolite with a pure **CON** phase is a borosilicate "CIT-1" (designated as [B]-CON) developed in 1995.[18] The **CON**-type aluminosilicate zeolite has also been synthesized by the postsynthesis method using deboronated [B]-CON.[18,19] The **CON**-type zeolite has been expected to show remarkable properties in the fields of catalysis and adsorption because of its unique structure with high accessibility and diffusibility; the 12- and 10-MR channels connect to form a large void at the intersections, providing access to the crystal interior through two pores.[19,20] Despite the attractive capabilities of the **CON**-type zeolites, a route for directly preparing **CON**-type aluminosilicate zeolites has not been developed.

We have developed the method for directly synthesizing Al-containing **CON**-type borosilicate zeolites, which are designed as [Al,B]-CON-D. They have proved to give an excellent catalytic performance in the MTO reaction. The differences in the acidic properties and catalytic performance between the directly- and postsynthesized **CON**-type aluminosilicate zeolites were also investigated in detail.

2. EXPERIMENTAL SECTION

2.1. Preparation of the CON-type Zeolites. *N,N,N*-Trimethyl-(−)-*cis*-myrtanylammonium hydroxide (TMMAOH), which was used as an organic structure-directing agent (OSDA) for crystallizing the **CON**-type zeolite, was prepared by methylation of (−)-*cis*-myrtanylamine (Aldrich)

Received: December 23, 2014
Revised: June 3, 2015
Published: June 4, 2015

DOI: 10.1021/acscatal.5b00692
ACS Catal. 2015, 5, 4268−4275

with methyl iodide (Wako) followed by ion-exchange treatment using SA10A−OH (Mitsubishi Chem.).

In a typical synthesis of [Al,B]-CON-D, boric acid (0.36 mmol, Wako) and aluminum sulfate (0.045 mmol, Wako) were added to the aqueous solution containing sodium hydroxide (0.9 mmol, Wako) and TMMAOH (1.8 mmol) with stirring. Fumed silica (9 mmol, Cab-O-Sil M7D, Cabot) as a silica source was added to the mixture. The molar composition of the resultant gel was $1SiO_2$:$0.04H_3BO_3$:$0.005Al_2(SO_4)_3$:0.1NaOH:0.2TMMAOH:$60H_2O$. Then, 2 wt % of as-made ***BEA**-type borosilicate ([B]-Beta), which was hydrothermally synthesized according to the previous report,[21] as seeds was added to the mixture. Thus, prepared mother gel was crystallized in an oven at 170 °C for 21 days under static conditions. The mother gel was also crystallized in an oven at 160 °C for 16 days under tumbling conditions (40 rpm). The solid product was recovered by filtration, washed with distilled water, and dried overnight at 100 °C. The obtained as-synthesized sample was calcined in the air at 600 °C for 6 h to remove organic moieties. To obtain H-type zeolites, the calcined Na-type ones were treated with 2 M NH_4NO_3 aq. at 80 °C for 1 h twice, followed by calcination at 600 °C for 6 h to exchange Na^+ ions for protons. The product was designated as "[Al,B]-CON-D (109, static)" when the zeolite was directly synthesized under the static conditions (the number in parentheses is the Si/Al atomic ratio in the product).

As a control, the **CON**-type aluminosilicate zeolite was synthesized by the postsynthesis method ([Al]-CON-P) as follows. First, the **CON**-type borosilicate ([B]-CON) was hydrothermally synthesized by using TMMAOH at 150 °C for 21 days according to the previous report.[18] The deboronation of [B]-CON (Si/B = 22) was conducted by the acid treatment using 0.01 M HCl for 24 h at 130 °C. The deboronated sample (Si/B = 453) was treated in the aqueous solution containing aluminum nitrate (Wako) for 12 h at 130 °C with the molar ratios of $1SiO_2$:$0.32Al(NO_3)_3$:$167H_2O$. In addition, ZSM-5 and Beta catalyst were used as a control. ZSM-5 (Si/Al = 149) was synthesized by hydrothermal synthesis according to the previous report as a reference.[22] For Beta, a commercial Beta (JRC-Z-HB150, Clariant Catalysts, Si/Al = 75) was used.

2.2. Characterizations. Powder X-ray diffraction (XRD) patterns were collected on a Rigaku Ultima III using a Cu Kα X-ray source (40 kV, 20 mA). FE-SEM images of the samples were obtained on a Hitachi S-5200 microscope operated at 1 kV. The samples on a carbon tape were observed without any metal coating. Elemental analysis of the samples (Si/Al ratio) was performed on an inductively coupled plasma-atomic emission spectrometer (ICP-AES, Shimadzu ICPE-9000). Temperature-programmed NH_3 desorption (NH_3-TPD) profiles were recorded on a BELCAT (BEL Japan). A thermal conductivity detector (TCD) was used to monitor desorbed NH_3. The amount of acidic sites was determined by using the area of the so-called "*h*-peak" in the profiles.[23,24]

The high-resolution ^{27}Al MAS NMR and ^{27}Al 3Q MQMAS NMR spectra of the H-type zeolites, which contained about 3% water, were obtained on a JEOL ECA-600 spectrometer (14.1 T) equipped with an additional 1 kW power amplifier using a ZrO_2 rotor (4 mm in size) under ambient conditions. For ^{27}Al 3Q MQMAS NMR spectra, the 3Q excitation pulse and the 3Q-1Q conversion pulse were 5.5 and 2.1 μs, respectively, and z-filter was 0.2 ms. The relaxation delay time was 10 ms. The ^{27}Al chemical shift was referenced to $AlNH_4(SO_4)_2\cdot 12H_2O$ at −0.54 ppm, and samples were spun at 17 kHz by using a 4 mm ZrO_2 rotor.

2.3. MTO Reaction. The MTO reaction, which gives ethene (C2=), propene (C3=), butenes (C4=), paraffins (C1−C4), over-C5 hydrocarbons, and dimethyl ether (DME) as products, was carried out in a fixed bed reactor. The reaction products were analyzed by an online gas chromatograph (GC-2014, Shimadzu) equipped with HP-PLOT/Q capillary column and an FID detector. The selectivities of the products were calculated on the carbon number basis. The reaction was performed at 500 °C at a W/F (weight/flow; the weight of catalyst (g) divided by the flow rate of liquid methanol (mol h^{-1}) fed into the reaction system) of 6.6 g h mol^{-1}. Typically, 50 mg of catalyst was calcined prior to the reaction at 520 °C for 1 h, and then the reactor was cooled to the desired reaction temperatures. As a control, commercial Beta (JRC-Z-HB150, Clariant Catalysts, Si/Al = 75) and hydrothermally prepared ZSM-5 (Si/Al = 149)[22] were tested for the MTO reaction.

3. RESULTS AND DISCUSSION

3.1. Preparation of the CON-type Zeolites. *3.1.1. Direct-Synthesis Method.* We attempted to directly incorporate Al atoms into the **CON** framework in the absence of boron atoms ([Al]-CON-D). Aluminum sulfate as an Al source was introduced into the mother gel in place of boric acid, and the hydrothermal treatment was conducted under the same conditions as [B]-CON, which can be obtained after the hydrothermal treatment of the mother gel with the Si/B atomic ratio of 25 at 150 °C for 21 days under static conditions.[18] The XRD pattern of the product indicated the diffraction peaks due to both an amorphous halo and the **CON** zeolite (Figure S1). Although the composition of the mother gel and the conditions of the hydrothermal treatment as well as the Al source were greatly altered, the synthesis of the zeolite with a pure **CON** phase was unsuccessful. These results imply that boron as well as the $TMMA^+$ cation plays an important role in the formation of the **CON**-type zeolite. Hereupon, we have focused on the addition of the Al source into the mother gel for preparing [B]-CON.

The product with a pure **CON** phase was not obtained from the mother gel containing both Al and B sources even when the hydrothermal treatment at 150 °C was extended to over 21 days. Therefore, the temperature was increased to 170 °C. At the atomic ratio of Si/B = 25 in the mother gel, the synthesis of [Al, B]-CON-D was conducted with the Al content varied. The mother gels with the Si/Al ratio below 100 did not give a pure **CON** phase (Figure 1a and b). However, when the Si/Al ratio in the mother gel was increased to 100, the **CON**-type zeolite with the Si/Al ratio of 117 was purely obtained after 21 days (Figure 1c). The mother gels with the Si/Al ratios of 150 and 200 also led to the formation of the **CON**-type zeolite (Figure 1d and e). The intensities of the peaks were slightly increased with a decrease in the Al source added. The physicochemical properties of the H-type samples are summarized in Table 1, indicating that the BET surface area and micropore volume of the **CON**-type aluminosilicate zeolites are comparable to those of [B]-CON (662 m^2 g^{-1} and 0.26 cm^3 g^{-1}).

3.1.2. Optimization of synthesis conditions for the CON-type zeolites. The synthesis conditions for the CON-type zeolites were investigated. We have also found that [Al,B]-CON-D can be synthesized in a shorter period and at a lower temperature by carrying out the hydrothermal treatment under tumbling conditions (40 rpm); the mother gels with the Si/Al

DOI: 10.1021/acscatal.5b00692
ACS Catal. 2015, 5, 4268−4275

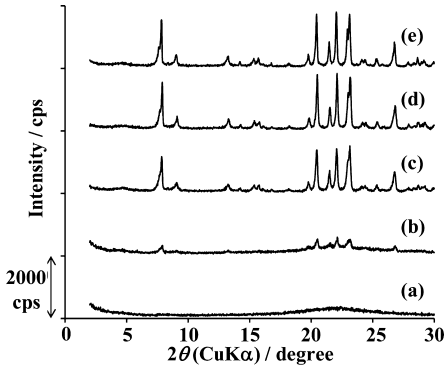

Figure 1. XRD patterns of aluminoborosilicate products by direct synthesis under static conditions with a Si/Al ratio of (a) 70, (b) 80, (c) 100, (d) 150, and (e) 200 in the mother gel. Mother gel composition is $1SiO_2$:$0.04H_3BO_3$: 0.0072−0.0025$Al_2(SO_4)_3$:0.1NaOH:0.2TMMAOH:60H_2O.

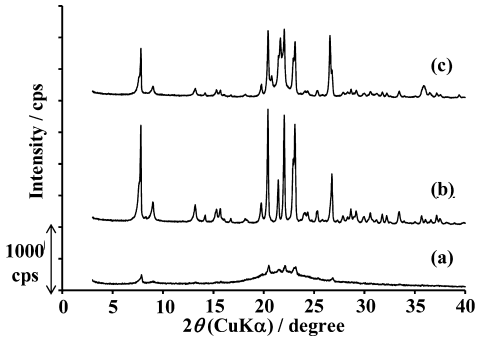

Figure 2. XRD patterns of aluminosilicate products synthesized at 200 °C for (a) 18 h, (b) 20 h, and (c) 48 h. Mother gel composition is $1SiO_2$:$0.04H_3BO_3$:$0.005Al_2(SO_4)_3$:0.1NaOH:0.2TMMAOH:20H_2O.

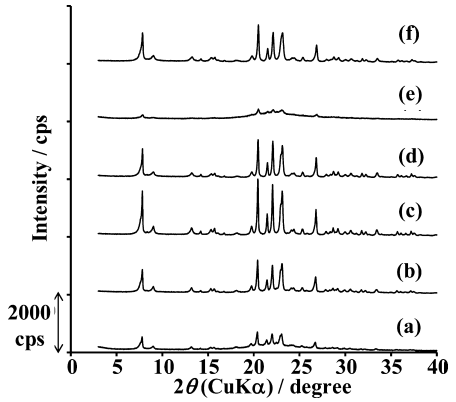

Figure 3. XRD patterns of aluminoborosilicate products synthesized with a Si/B ratio of (a) 100, (b) 50, (c) 25, (d) 13 (e) 10, and (f) 10 with Na/Si ratio of 0.12. Mother gel composition is $1SiO_2$:0.01−$0.1H_3BO_3$:$0.0025Al_2(SO_4)_3$:0.1NaOH:0.2TMMAOH:30H_2O.

ratio ranging from 100 to 200 were purely crystallized into the **CON**-structure at 170 °C after 16 days (Figure S2a and b).

Furthermore, we succeeded in crystallizing the **CON**-type zeolite in only 20 h by increasing the temperature to 200 °C and decreasing the H_2O/Si ratio from 60 to 20. Note that, when the crystallization was carried out at 200 °C, the phase obtained was very sensitive to the duration of crystallization. The **CON**-phase appeared in 18 h (Figure 2a), and then a pure **CON**-phase was obtained 20 h after (Figure 2 (b)), but it was changed to other phases in 48 h (Figure 2c). Further investigations on the effect of the temperature of the hydrothermal treatment are currently under way.

The effect of the boron content on the crystallization of the **CON**-type zeolite was investigated under tumbling conditions at 170 °C with the Si/Al in the gel constant at 200 (Figure 3). When the Si/B ratios in the mother gel ranged from 13 to 50, the zeolite with a pure **CON** phase was obtained. For these Si/B ratios, the Si/B ratios in the products ranged from 20 to 40, and the Si/Al ratios were nearly constant at about 200, irrespective of the B content. From the mother gel with the Si/B ratio at 10, the crystallization slightly occurred; amorphous phases were mainly observed in the XRD pattern (Figure 3e). However, the **CON**-type zeolite was purely crystallized by increasing the Na/Si ratio from 0.1 to 0.12 (Figure 3f), suggesting that the strong alkalinity enhances the crystallization. On the other hand, when the Si/B ratio in the mother gel was increased to 100, the intensities of the diffraction peaks due to the **CON** type zeolite were drastically decreased (Figure 3a). Further hydrothermal treatment enhanced the formation of a dense silica product, cristobalite, not the **CON**-type zeolite. The crystallization of the **CON**-type zeolite in the absence of B was still unsuccessful under the tumbling conditions at 170 °C.

These findings suggest that the crystallization of the **CON**-type zeolite is strongly dependent on the crystallization temperature, the B content and the alkalinity, and that the increase in the Al content retards the crystallization.

3.1.3. Postsynthesis Method. First, the **CON**-type aluminosilicate was prepared using the postsynthesis method

Table 1. Physicochemical Properties of the CON-type Zeolite Materials, Beta and ZSM-5

		Si/B		Si/Al					
sample	system	gel	product	gel	product	S_{BET} [a] ($m^2 \cdot g^{-1}$)	S_{ex} [b] ($m^2 \cdot g^{-1}$)	V_{micro} [c] ($m^3 \cdot g^{-1}$)	A_{acid} [d] ($mmol \cdot g^{-1}$)
[Al,B]-CON-D	static	25	37	100	109	630	9	0.25	0.12
[Al,B]-CON-D	static	25	28	150	144	595	33	0.23	0.07
[Al,B]-CON-D	static	25	25	200	196	589	20	0.21	0.06
[Al,B]-CON-D	tumbling	25	26	100	134	665	88	0.24	0.06
[Al,B]-CON-D	tumbling	25	34	200	155	659	125	0.23	0.05
[B]-CON	static	25	22			662	11	0.26	
[-]-CON			453			651	20	0.25	
[Al]-CON-P			n.d.		87	637	23	0.23	0.06
Beta					75	685	181	0.20	0.22
ZSM-5				150	149	454	16	0.24	0.09

[a] S_{BET}: BET surface area, [b] S_{ex}: external surface area, [c] V_{micro}: micropore volume, [d] A_{acid}: acid amount based on the NH_3-TPD measurements

DOI: 10.1021/acscatal.5b00692
ACS Catal. 2015, 5, 4268−4275

(designed as [Al]-CON-P), which includes the deboronation followed by the Al insertion processes.[18] The XRD patterns indicated that the **CON** structure remained after the Al incorporation using aluminum nitrate (Figure S3). The Si/B ratio was increased from 22 to 453 via the deboronation. In the Al insertion process, the boron content was further decreased to a level undetectable by the ICP analysis.

3.2. Structural Properties of the CON-type Aluminosilicate Zeolites. The FE-SEM images revealed that crystals of acuate-square prisms 2−4 μm in length were present in the [Al,B]-CON-D samples synthesized under static conditions, while [B]-CON consisted of acuate-square prisms 1−2 μm in length (Figure 4). The particle size of [Al]-CON-P (87) was smaller than that of the [Al,B]-CON-D samples. The morphology of [Al,B]-CON-D synthesized under tumbling conditions was slightly different from that of the samples synthesized under the static conditions; a stack of smaller-sized particles was observed in the crystals of acuate-square prisms.

Figure 5 shows the ^{27}Al MAS MNR spectra of the products. A strong and broad peak at 54−59 ppm is assigned to

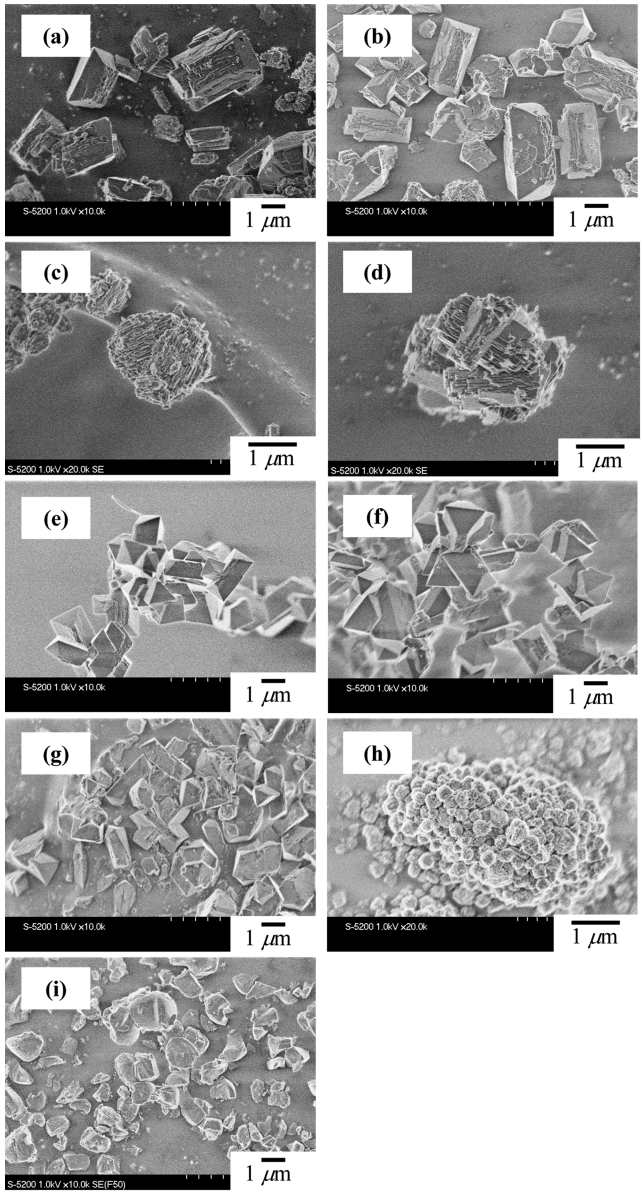

Figure 4. SEM images of (a) [Al,B]-CON-D (109, static), (b) [Al,B]-CON-D (196, static) (c) [Al,B]-CON-D (134, tumbling), (d) [Al,B]-CON-D (155, tumbling), (e) [B]-CON, (f) [−]-CON, (g) [Al]-CON-P (87), (h) Beta, and (i) ZSM-5.

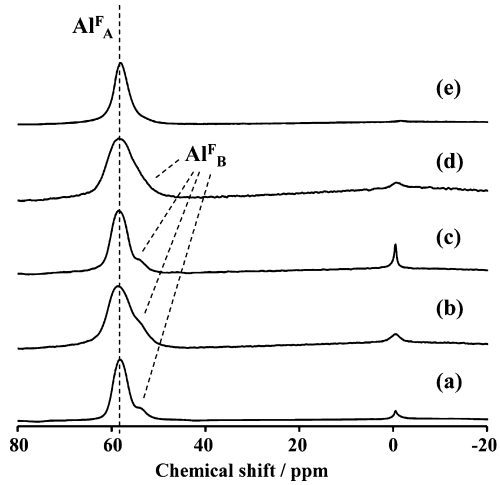

Figure 5. ^{27}Al MAS NMR spectra of (a) [Al,B]-CON-D (109, static), (b) [Al,B]-CON-D (196, static), (c) [Al,B]-CON-D (134, tumbling), (d) [Al,B]-CON-D (155, tumbling), and (e) [Al]-CON-P (87).

tetrahedrally coordinated Al species irrespective of the preparation routes. Except for [Al]-CON-P (87), a small peak at −0.6 ppm assigned to octahedrally coordinated Al species was also observed. Note that, for the directly synthesized **CON**-type zeolites, the main peak clearly consists of two peaks; the major peak appeared at 58 ppm, and a shoulder peak at 55 ppm (Figure 5a−d). The shoulder peak at 55 ppm in the ^{27}Al MAS NMR spectra might be assigned to tetrahedrally coordinated Al species in the framework and/or extra-framework. These findings suggest that there is a significant difference in the environment of Al species, e.g., the location of Al atom in the framework, between the directly- and postsynthesized **CON**-type zeolites.

The acidity of the samples was examined by NH_3-TPD (Figure 6). The temperature for *h*-peak, corresponding to NH_3 desorption from catalytically active BASs and LASs,[23,24] was estimated at 341, 330, 328, 323, 324, 344, and 363 °C for [Al,B]-CON-D (109, static), [Al,B]-CON-D (196, static), [Al,B]-CON-D (134, tumbling), [Al,B]-CON-D (155, tumbling), [Al]-CON-P (87), Beta (75), and ZSM-5 (149) (the number in the parentheses is the Si/Al ratio in the product), respectively, indicating that the acidic strength of the **CON**-type zeolites is slightly weaker than that of Beta. [Al]-CON-P showed an *h*-peak at a lower temperature than the [Al,B]-CON-D samples, indicating that the acidic strength is dependent on the preparation method.

In order to clarify the difference in the acidic properties, the FT-IR spectra of adsorbed pyridine were measured after evacuation at 150 °C (Figure S4). The absorption peaks of pyridine adsorbed on Lewis and Brønsted acid sites appeared at 1455 and 1544 cm^{-1}, respectively. [Al]-CON-P (87) has a higher proportion of Lewis acid sites than [Al,B]-CON-D (109, static); the proportion of Brønsted acid sites to Lewis acid sites (B/L ratio) for [Al,B]-CON-D (109, static) and [Al]-CON-P (87) were estimated at 13 and 5.8, respectively. A large amount of Lewis acid sites on [Al]-CON-P (87) would be derived from the extra-framework Al species. Unfortunately, attempts to

DOI: 10.1021/acscatal.5b00692
ACS Catal. 2015, 5, 4268−4275

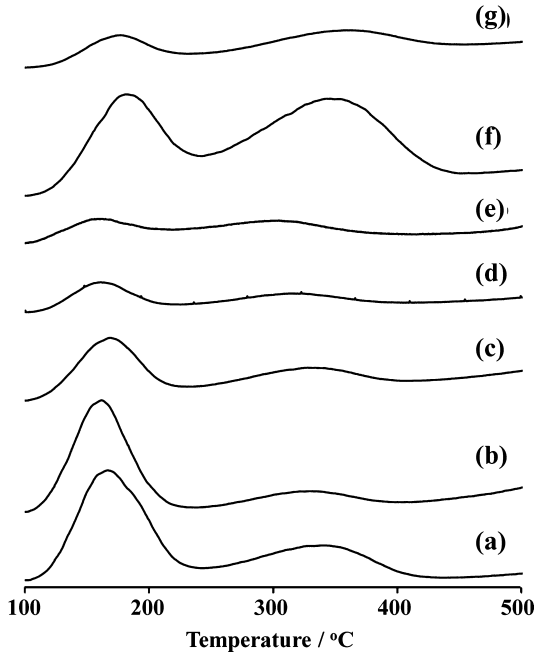

Figure 6. NH_3-TPD profiles of (a) [Al,B]-CON-D (109, static), (b) [Al,B]-CON (196, static), (c) [Al,B]-CON (134, tumbling), (d) [Al,B]-CON (155, tumbling), (e) [Al]-CON-P (87), (f) Beta (75), and (g) ZSM-5 (149).

elucidate the difference in the acidic strength of the samples by using pyridine adsorbed FT-IR were unsuccessful because of the low amount of acidic sites.

3.3. Catalytic Performance of the CON-type Aluminosilicate Zeolites in the MTO Reaction. Thus, prepared **CON**-type aluminosilicate zeolites were used as catalysts for the MTO reaction. Figure 7 shows the change in the conversion of methanol and the product selectivity along with time on stream (TOS) at 500 °C. For the **CON**-type zeolite catalysts, at the initial stage (time = 10 min), the conversion of methanol was ca. 100%, the main product was propene, and its selectivity reached 50% (Figure 7a–d). Butenes were formed with a selectivity of about 20%; among butenes, the selectivities to isobutene, 1-butene, and *trans*-2- and *cis*-2-butenes were about 10, 25, 40 and 25%, respectively. Note that the selectivity to ethene was as low as 5%.

Interestingly, the directly synthesized **CON**-type aluminosilicate zeolites showed a much longer catalytic life than the zeolite synthesized by the postsynthesis method. For [Al]-CON-P (87), although the conversion of methanol and the selectivity to propene were 99 and 50% at the initial stage, respectively, these values were remarkably decreased to 81 and 35%, respectively, at a TOS of 10 h. Instead of the decrease in the selectivity to propene, dimethyl ether (DME) was rapidly increased at a TOS of 7 h (Figure 7 (d)). On the other hand, [Al,B]-CON-D (109, static) gave a 100% conversion of methanol and a 60% selectivity to propene even at a TOS of 10 h. Butenes were constantly formed with a selectivity of about 20% for 16 h. The selectivity to ethene was hardly changed; it was kept less than 5% for 16 h. For a higher-silica type sample, [Al,B]-CON-D (196, static), the 100% conversion was kept for 16 h with the products' selectivities unchanged.

The very low selectivity to ethene on the **CON**-type aluminosilicate zeolites might be accounted for as follows. Based on the "dual-cycle concept" proposed by Olsbye and her co-workers[1,25] for the conversion of methanol, the low acid strength of the **CON**-type zeolites contributes to the suppression of aromatization of higher alkenes formed in the alkene methylation/cracking cycle. They also proposed that ethene is formed from the "aromatics-based cycle." Therefore, the use of the **CON**-type zeolites would result in lessened formation of ethene. The three-dimensional large pores system with a high diffusibility would also suppress sequential reactions, oligomerization, and the following cracking, in the pores, leading to the low selectivity to ethene. More interestingly, the **CON**-type zeolite synthesized under tumbling conditions ([Al,B]-CON-D (134, tumbling)) exhibited a much longer catalytic life than those synthesized under static conditions; the 100% conversion was kept for 24 h with the selectivity to propene of about 60% unchanged, and the total selectivity for C3–C4 olefins was kept at about 80%. The differences between the static and tumbling conditions in the direct synthesis were crystallization time, particle morphology and Al distribution in the framework. It is well-known that particle sizes of catalysts affect the catalytic life for the MTO reaction; a smaller-sized catalyst generally exhibited a longer catalytic life than a larger-sized one.[2,26] However, the catalytic life of [Al]-CON-P (87) was significantly short despite the smaller particle. We have considered that, in addition to particle morphology, the Al distribution in the framework strongly affected the catalytic performance (see section 3.4).

Beta (75) showed the 100% conversion and the propene selectivity of 63% at the initial stage. However, this high performance was retained for only 4 h, and the deactivation progressed along with TOS. For ZSM-5 (149), the conversion of methanol and the selectivity to propene were 100 and 50%, respectively. The selectivity to ethene at the initial stage (ca. about 10%) was higher than that of other zeolites investigated. The catalytic life of ZSM-5 was slightly longer than the postsynthesized **CON**- and ***BEA**-type zeolites; however, it was much shorter than that of the directly synthesized **CON**-type zeolite.

3.4. Difference in the Al Distribution between the Directly and Postsynthesized CON-type Zeolites. We have found that there is a marked difference in the catalytic activity between the direct and postsynthesis methods, and that there is also a significant difference in the catalytic activity between the static and tumbling conditions in the direct synthesis. The factors for affecting the catalytic performance were considered as follows.

It has been reported that the defect sites (≡Si–OH groups) and Lewis acid sites affect the activity in the MTO reaction, in particular the formation of aromatics.[27,28] Based on the FT-IR spectra of adsorbed pyridine (Figure S4), we have confirmed that [Al]-CON-P (87) has a higher proportion of Lewis acid sites than [Al,B]-CON-D (109, static). The ^{29}Si MAS and CP/MAS NMR spectra of [Al,B]-CON-D (106, static) and [Al]-CON-P (87) (Figures S5 and S6) suggest that the number of defect sites in [Al]-CON-P (87) was slightly higher than that in [Al,B]-CON-D (106, static). In addition to Lewis acid and defect sites and particle morphology, we have considered that the Al distribution in the **CON** framework also has a significant influence on the catalytic performance.

The **CON**-type zeolite consists of a three-dimensional channel system with 12-, 12-, and 10-MR pores. In the direct-synthesis method, Al atoms might be uniformly introduced into the zeolite framework. On the other hand, in the postsynthesis method, considering the size of hydrated Al

DOI: 10.1021/acscatal.5b00692
ACS Catal. 2015, 5, 4268–4275

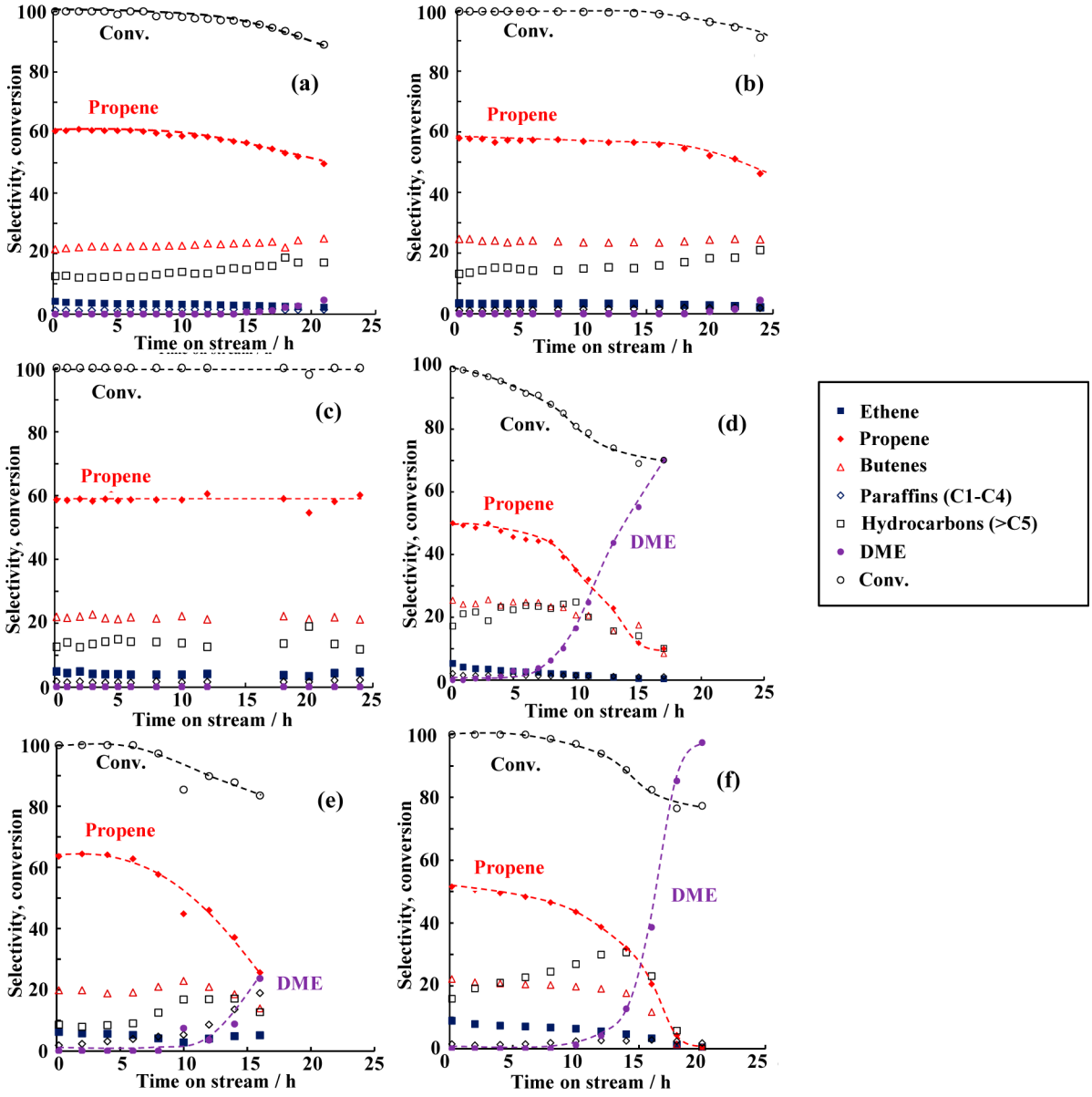

Figure 7. MTO reaction results at 500 °C over (a) [Al,B]-CON-D (109, static), (b) [Al,B]-CON-D (196, static), (c) [Al,B]-CON-D (134, tumbling), (d) [Al]-CON-P (87), (e) Beta (75), and (f) ZSM-5 (149). Reaction conditions: 50 mg catalyst, 12.5% MeOH diluted in He, W/F = 6.6 g·h/mol, 500 °C.

species, $[Al(H_2O)_6]^{3+}$ (about ~6 Å in length),[29] existing under the synthesis conditions, Al species might be preferentially inserted into larger pores, i.e. 12-MR rather than 10-MR pores. Very recently, Zones et al. reported the Al reinsertion into borosilicate zeolites with intersecting channels of 10- and 12-MR pore systems. For B-SSZ-57, which has 12-MR and 10-MR pores, Al atoms are selectively incorporated into the framework of the 12-MR pore because the 12-MR pore of SSZ-57 is independent of the 10-MR pore.[30,31] On the other hand, they concluded that SSZ-33, which is a **CON**-family zeolite, Al atoms are introduced into all of the vacancy sites formed by deboronation.[31,32] The Al content of [Al]-CON-P (87) was not high enough to occupy all of the vacancy sites, because it is much lower than the decrease of the B content upon Al incorporation. It would be reasonable to assume that acid sites would be concentrated on the 12-MR pores where the aromatization of the once formed alkenes mainly occurred. The higher selectivity for heavy compounds and the lower selectivity to propene observed for [Al]-CON-P (87) might be explained on this hypothesis.

The ^{27}Al MAS NMR spectra indicate that the **CON**-type zeolite has at least two kinds of different Al species. To clarify the difference in the Al distribution between the directly and postsynthesized **CON**-type zeolites, the high resolution ^{27}Al 3Q MQMAS NMR spectra were measured (Figure 8). In the ^{27}Al MQMAS NMR spectra, the spectra of the samples directly prepared under the static conditions clearly showed two cross sections, designated as "a" and "b" (Figures 8a and b). For the sample directly prepared under the tumbling conditions, [Al,B]-CON-D (134, tumbling), in addition to "a" and "b", the cross-section "c" was newly observed (Figure 8c). Note that only one cross-section "a" was observed in the spectrum of [Al]-CON-P (87) (Figure 8d).

Deng et al. reported that the cross sections due to four-coordinated and five-coordinated extra-framework Al (EFAL) species in the dealuminated HY zeolite can be observed in ^{27}Al

DOI: 10.1021/acscatal.5b00692
ACS Catal. 2015, 5, 4268−4275

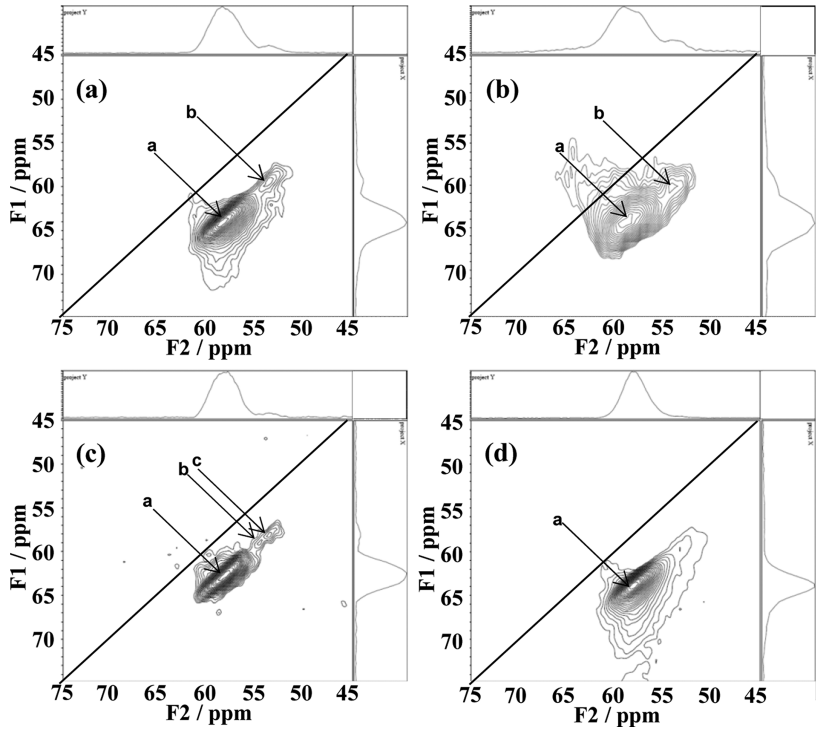

Figure 8. ^{27}Al MQMAS NMR spectra of (a) [Al,B]-CON-D (106, static), (b) [Al,B]CON-D (196, static), (c) [Al,B]-CON-D (134, tumbling), and (d) [Al]-CON-P (87).

MQMAS and DQMAS NMR, but these peaks disappeared at the high water loading.[33,34] In our case, the three cross sections "a," "b," and "c" in the ^{27}Al MQMAS NMR spectra were observed parallel to the CS axis and the three cross sections due to the four- and five-coordinated EFAL species were hardly observed (Figure 8). Based on these facts, it could be concluded that the cross sections "a," "b," and "c" in the ^{27}Al MQMAS NMR spectra are derived from the tetrahedrally coordinated Al species in the framework.

These findings indicate that there is a marked difference in the state of tetrahedrally coordinated Al species in the framework between the directly and postsynthesized zeolites, and that there is also a significant difference in the Al distribution among the samples directly prepared under the static and tumbling conditions. We consider that the framework Al atoms corresponding to the cross sections "b" and "c" contribute to the suppression of the formations of aromatics and heavy hydrocarbons. The presence of the framework Al atom "c" and small particle could explain the reason for the long catalytic life of [Al,B]-CON-D (134, tumbling) compared with [Al,B]-CON-D synthesized under static conditions.

4. CONCLUSIONS

In conclusion, the **CON**-type aluminosilicate zeolite was successfully synthesized by the direct-synthesis methods as well as the postsynthesis ones. The ^{27}Al 3Q MQMAS measurements revealed that the preparation method has a marked influence on the Al distribution in the **CON** framework. We found a unique catalytic performance of the **CON**-type zeolites in the MTO reaction. In particular, the **CON**-type aluminosilicate zeolites directly prepared under the tumbling conditions exhibited a high propene selectivity, low ethene selectivity, and a very long catalytic life compared to Beta and ZSM-5, and the total selectivity for C3−C4 olefins of 80% was achieved. In addition to Lewis acid and defect sites and particle morphology, we have considered that the Al distribution in the **CON** framework also has a significant influence on the catalytic performance. Our findings will contribute to the development of the zeolite catalysts with acid sites in the pores properly controlled and would broaden catalytic applications of the **CON**-type zeolites.

■ ASSOCIATED CONTENT

Supporting Information

The following file is available free of charge on the ACS Publications website at DOI: 10.1021/acscatal.5b00692.

Figures S1−S6 and Table S1 (PDF)

■ AUTHOR INFORMATION

Corresponding Author

*Fax: +81-45-924-5282. E-mail: yokoi@cat.res.titech.ac.jp.

Notes

The authors declare no competing financial interest.

■ ACKNOWLEDGMENTS

We thank Dr. Tooru Setoyama (Mitsubishi Chemical Group, Science and Technology Research Center) for helpful discussion. This work was partially supported by Japan Technological Research Association of Artificial Photosynthetic Chemical Process (ARPChem).

■ REFERENCES

(1) Olsbye, U.; Svelle, S.; Bjørgen, M.; Beato, P.; Janssens, T. V. W.; Joensen, F.; Bordiga, S.; Lillerud, K. P. *Angew. Chem., Int. Ed.* **2012**, *51*, 5810−5831.
(2) Tian, P.; Wei, Y.; Ye, M.; Liu, Z. *ACS Catal.* **2015**, *5*, 1922−1938.
(3) Plotkin, J. S. *Catal. Today* **2005**, *106*, 10−14.

DOI: 10.1021/acscatal.5b00692
ACS Catal. 2015, 5, 4268−4275

(4) Chen, J. Q.; Bozzano, A.; Glover, B.; Fuglerud, T.; Kvisle, S. *Catal. Today* **2005**, *106*, 103−107.
(5) Chang, C. D.; Chu, C. T.-W.; Socha, R. F. *J. Catal.* **1984**, *86*, 289−296.
(6) Zhu, Q.; Kondo, J. N.; Tatsumi, T.; Inagaki, S.; Ohnuma, R.; Kubota, Y.; Shimodaira, Y.; Kobayashi, H.; Domen, K. *J. Phys. Chem. C* **2007**, *111*, 5409−5415.
(7) Zhu, Q.; Kondo, J. N.; Ohnuma, R.; Kubota, Y.; Yamaguchi, M.; Tatsumi, T. *Microporous Mesoporous Mater.* **2008**, *112*, 153−161.
(8) Zhu, Q.; Hinode, M.; Yokoi, T.; Kondo, J. N.; Kubota, Y.; Tatsumi, T. *Microporous Mesoporous Mater.* **2008**, *116*, 253−257.
(9) Park, J. W.; Lee, J. Y.; Kim, K. S.; Hong, S. B.; Seo, G. *Appl. Catal., A* **2008**, *339*, 36−44.
(10) Zhu, Q.; Hinode, M.; Yokoi, T.; Yoshioka, M.; Kondo, J. N.; Tatsumi, T. *Catal. Commun.* **2009**, *10*, 447−450.
(11) Yokoi, T.; Yoshioka, M.; Imai, H.; Tatsumi, T. *Angew. Chem., Int. Ed.* **2009**, *48*, 9884−9887.
(12) Kumita, Y.; Gascon, J.; Stavitski, E.; Moulijn, J. A.; Kapteijn, F. *Appl. Catal., A* **2011**, *391*, 234−243.
(13) Bleken, F.; Skistad, W.; Barbera, K.; Kustova, M.; Bordiga, S.; Beato, P.; Lillerud, K. P.; Svelle, S.; Olsbye, U. *Phys. Chem. Chem. Phys.* **2011**, *13*, 2539−2549.
(14) Wang, Q.; Cui, Z.-M.; Cao, C.-Y.; Song, W. G. *J. Phys. Chem. C* **2011**, *115*, 24987−24992.
(15) Dorset, D. L.; Weston, S. C.; Dhingra, S. S. *J. Phys. Chem. B* **2006**, *110*, 2045−2050.
(16) Lobo, R. F.; Pan, M.; Chan, I.; Li, H. X.; Medrud, R. C.; Zones, S. I.; Crozier, P. A.; Davis, M. E. *Science* **1993**, *262*, 1543−1546.
(17) Lobo, R. F.; Pan, M.; Chan, I.; Medrud, R. C.; Zones, S. I.; Crozier, P. A.; Davis, M. E. *J. Phys. Chem.* **1994**, *98*, 12040−12052.
(18) Lobo, R. F.; Davis, M. E. *J. Am. Chem. Soc.* **1995**, *117*, 3766−3779.
(19) Mathew, T.; Elangovan, S. P.; Yokoi, T.; Tatsumi, T.; Ogura, M.; Kubota, Y.; Shimojima, A.; Okubo, T. *Microporous Mesoporous Mater.* **2010**, *129*, 126−135.
(20) Elangovan, S. P.; Ogura, M.; Davis, M. E.; Okubo, T. *J. Phys. Chem. B* **2004**, *108*, 13059−13061.
(21) de Ruite, R.; Famine, K.; Kentgens, A. P. M.; Jansen, J. C.; van Bekkum, H. *Zeolites* **1993**, *13*, 611−621.
(22) Argauer, R. J.; Landolt, G. R. U.S. Patent 3,702,886, 1972.
(23) Niwa, M.; Katada, N. *Catal. Surv. Jpn.* **1997**, *1*, 215−226.
(24) Suzuki, K.; Aoyagi, Y.; Katada, N.; Choi, M.; Ryoo, R.; Niwa, M. *Catal. Today* **2008**, *132*, 38−45.
(25) Bjørgen, M.; Svelle, S.; Joensen, F.; Nerlov, J.; Kolboe, S.; Bonino, F.; Palumbo, L.; Bordiga, S.; Olsbye, U. *J. Catal.* **2007**, *249*, 195−207.
(26) Yang, G.; Wei, Y.; Xu, S.; Chen, J.; Li, J.; Liu, Z.; Yu, J.; Xu, R. *J. Phys. Chem. C* **2013**, *117*, 8214−8222.
(27) Sazama, P.; Wichterlova, B.; Dedecek, J.; Tvaruzkova, Z.; Musilova, Z.; Palumbo, L.; Sklenak, S.; Gonsiorova, O. *Microporous Mesoporous Mater.* **2011**, *143*, 87−96.
(28) Barbera, K.; Bonino, F.; Bordiga, S.; Janssens, T. V. W.; Beato, P. *J. Catal.* **2011**, *280*, 196−205.
(29) Persson, I. *Pure Appl. Chem.* **2010**, *82*, 1901−1917.
(30) Zones, S. I.; Chen, C. Y.; Benin, A.; Hwang, S.-J. *J. Catal.* **2013**, *308*, 213−225.
(31) Zones, S. I.; Benin, A.; Hwang, S. J.; Xie, D.; Elomari, S.; Hsieh, M.-F. *J. Am. Chem. Soc.* **2014**, *136*, 1462−1471.
(32) Chen, C. Y.; Zones, S. I.; Hwang, S.-J.; Bull, L. M. *Stud. Surf. Sci. Catal.* **2004**, *154*, 1547−1554.
(33) Li, S.; Zheng, A.; Su, Y.; Fang, H.; Shen, W.; Yu, Z.; Chen, L.; Deng, F. *Phys. Chem. Chem. Phys.* **2010**, *12*, 3895−3903.
(34) Yu, Z.; Zheng, A.; Wang, Q.; Chen, L.; Xu, J.; Amoureux, J.-P.; Deng, F. *Angew. Chem., Int. Ed.* **2010**, *49*, 8657−8661.

DOI: 10.1021/acscatal.5b00692
ACS Catal. 2015, 5, 4268−4275